ZIBELINE INTERNATIONAL™ PUBLISHING

Pakistan Journal of Geology (PJG)

DOI: http://doi.org/10.26480/pjg.01.2025.41.48

ISSN: 2521-2915 (Print)
ISSN: 2521-2923 (Online)
CODEN: PJGABN

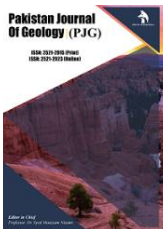

CrossMark

RESEARCH ARTICLE

WELL LOG SEQUENCE STRATIGRAPHY IN DETERMINING LITHOFACIES AND LITHO-FLUID VARIABILITY IN EASTERN NIGER DELTA BASIN, NIGERIA

Anwana, U. E., Akpabio, Idara O.

Department of Physics, Faculty of Physical Sciences, University of Uyo, Nigeria.
****Corresponding Author Email: mbereobong.archibong@nmu.edu.ng.***

ARTICLE DETAILS

Article History:

Received 24 May 2025
Revised 17 June 2025
Accepted 25 June 2025
Available online 01 July 2025

ABSTRACT

Investigation of the change in grain size distribution, pore fluid and lithologic association with respect to the influence of depositional environment was adopted to ascertain its imperativeness to hydrocarbon recovery. Suite of well logs (resistivity, gamma ray, density and neutron) from three wells, SB1, SB2 and SB3 were used to delineate lithologies and grain size distributions; identify fluid contact and volume of shale. Lithology and litho-fluid cross-plots show variability in lithofacies, while the two porosity logs (density and neutron) were used to compute porosity. In the three wells, the identified facies (funnel, cylindrical and bell shape trends) and litho-fluid cross-plot show gamma ray values ranging from 30 to 60 API; high resistivity values up to 1123 Ω-m; mean porosity value of 22% to 32%; mean shale volume of 0.06 to 0.24. The results show a good to excellent reservoir properties capable of supporting hydrocarbon exploration and production. The intermittent variability in lithofacies of coarsening upward and downward and lithologies is not unconnected with the discrete velocities of different grain sizes during transportation and subsequent differential drag forces during deposition. The wells correlation and the results obtained have deepened the sedimentological and stratigraphic knowledge of reservoir quality and continuity as a proof of good prospect.

KEYWORDS

Stratigraphy, Lithofacies, Lithologic variability, Well correlation.

1. INTRODUCTION

Exploration for economic reserves of hydrocarbon requires knowledge of the depositional history in the study area; to determine whether suitable source rocks are likely to have been formed and if there are any reservoir and cap lithologies in the overlying succession. Well log sequence stratigraphy is a sub-discipline of stratigraphy that involves the subdivision of sedimentary basin fills into genetic packages or genetically related strata, bounded at the top and base by chronostratigraphic surfaces called unconformities or correlative conformities (Reijers, 2011; Nuhu et al., 2019).

In order to understand the distribution of sedimentary facies in the subsurface, one need to view it as parts of depositional systems (Emery and Mayers, 1996). Using a combination of different datasets, it may be possible to understand the depositional systems well so as to enable geoscientists predict sand distribution, geometry, continuity and quality of reservoir. Sequence stratigraphy is therefore one of the important geologic tools in the interpretation process of sedimentation and depositional history within a basin. Geophysical well logs are commonly used for well correlation, lithology identification and formation evaluation. Currently, well log (gamma ray) shapes are being applied in facies analysis and in the determination of depositional environment (Nwagwu et al., 2019; Okoli et al., 2020). It provides a logical and useful aid in exploration of hydrocarbon, ranging from areas with restricted well control to exploration in mature areas with many production wells (Oyedele et al., 2012).

Integration of well log stratigraphic analysis in hydrocarbon exploration reveals subtle traps which require a multidisciplinary approach. Porosity enhancement can be detected through sequence stratigraphy analysis to improve reservoir quality in otherwise tight sections. Gamma ray log shows strong affinity to natural radioactivity of the formation, to determine rock types in a well. Shale has propensity to trap radioactive elements which are typically rich in clay mineral like glauconite, smectite and montmorillonite. The value of gamma ray log is therefore normally low in clean sandstones and high in shales signifying low and high API value respectively (Boggs, 2006).

Gamma ray log is also used to measure grain size and consequently inferring depositional energy; that is, a low energy environment or high energy environment. Thus, coarse-grained sand with little mud will have low gamma value, while a fine-grained lithology with a high mud content will have a high gamma ray value. Porous and permeable sands containing hydrocarbon will give high resistivity response while brine bearing sands and shales give low resistivity response.

Figure 1 shows the different gamma log responses to variation in grain sizes: bell shape (coarsening downward; funnel shape (coarsening upward; cylindrical or block shape (sharp top and base; bow or symmetrical (gradual coarsening downward) and a little fining downward; and irregular or serrated block (inconsistent in gamma response).

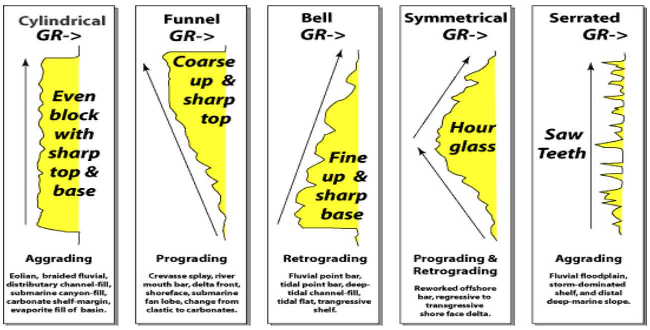

Figure 1: General gamma ray responses to variation in grain size

Source: Modified from Emery and Mayers (1996)

Quick Response Code	Access this article online	
	Website: www.pakjgeology.com	**DOI:** 10.26480/pjg.01.2025.41.48

Cite The Article: Anwana, U. E., Akpabio, Idara O. (2025). Well Log Sequence Stratigraphy in Determining Lithofacies and Litho-Fluid Variability in Eastern Niger Delta Basin, Nigeria. *Pakistan Journal of Geology, 9(1): 41-48.*

The gamma-ray log shapes are frequently used for interpreting sedimentary cycles or depositional facies and their environments. They differentiate geothermal zones in the Niger Delta using variation in bottom hole temperature (Akpabio et al., 2003; Akpabio et al., 2013). The five log trends are: bell shape (upwards increasing in gamma counts); funnel shape (upward decrease in gamma counts; box-car or cylindrical shape (relatively consistent gamma readings); bow shape (systematic increase and decrease in gamma counts); and irregular trend (no systematic charge in gamma values).

1.1 Recognition of Well Log Stacking Patterns and Parasequences

The morphology, log curves and the nature of the lower and upper boundaries with adjacent lithological units are used to determine the different log motifs. The depositional sequences arising from depositional patterns; episodes of transgression and regression; and attendant system tracts can be identified from log signatures. These are; Highstand System Tract (HST) which is the zone of high sea level rise that gives rise to coarsening upward trend on the log signature. Transgressive System Tracts (TST), deposited during sea level rise and is recognised on the log signatures as a bell shape facies (fining upward trend); Lowstand System Tract (LST) occurs during sea level fall and resulted in funnel shape facies (fining downward trend). It is the zone of prolific hydrocarbon exploration. The Maximum Flooding Surface (MFS) is the point of inflection of marine facies of pelagic deposits and identified by abundance of planktonic microfossils. The system tracts comprise an integration of depositional environments which form depositional sequences. They were delineated using standard log motif for gamma ray responses (fining upward or coarsening downward and fining downward or coarsening upward) of lithological units. The findings will be tied to the delta wide sequence stratigraphic facies, system tracts and environment of depositional chart presented by (Doust and Omatsola, 1990).

The study utilizes well log and porosity datatset to determine stratigraphic changes in lithofacies and litho-fluid within the reservoir as a function of depositional environment for prospect study.

1.2 Geology and Stratigraphic Setting of Study Area

Niger Delta is a marginal sag basin situated on the continental margin of the Gulf of Guinea in Equatorial West Africa. Basement tectonics related to crucial divergence and translation during the late Jurassic and Cretaceous continental rifting, probably determined the original site of the main rivers that controlled the early development of the Delta, with a maximum thickness of about 12,000m in the depocenter (Doust and Omatsola, 1990). From the Eocene to Recent, the delta has prograded South-West, forming depobelts that represent the most active portions of the delta at each state of its development. Figure 2 shows the study area.

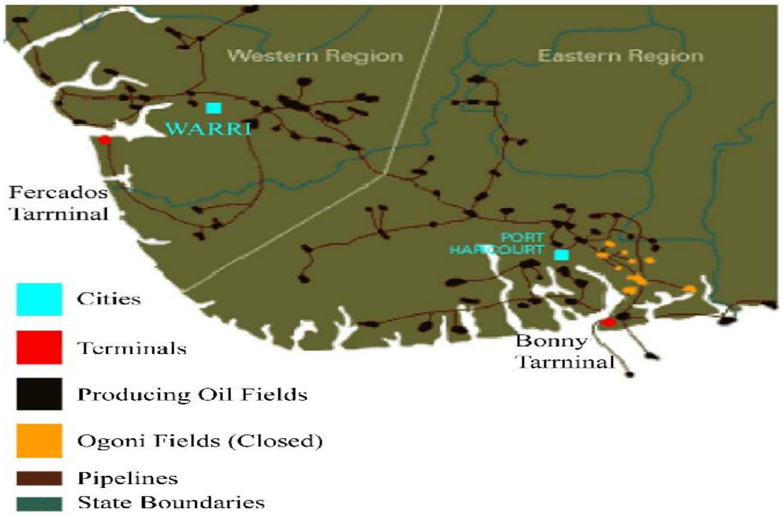

Figure 2: Map of the Study Area

The first coarse clastic deposits have been dated on the basis of micro floral units at early Eocene. Sediments show an upward transition from marine pro-delta shales (Akata Formation) through a paralic interval (Agbada Formation) to a continental sequence (Benin Formation). These three sedimentary formations, typical of most deltaic environments extend across the whole delta and range in age from early Tertiary to Recent (Ejedawe, 1989). Agbada Formation has been identified to accumulate economically exploitable quantity of hydrocarbon.

Structurally, the Niger Delta Shelf developed as a prograding extensional complex overlying a ductile substrate which composed largely of over pressured marine shales. Doust and Omatsola (1990), describe the most viable trapping system of the Niger delta to be the extensional growth faults located in the upper Agbada Formation (Ogwashi-Asaba). These structures formed as a result of gravity sliding during the course of early deltaic sedimentation.

2. Materials and Methods

The study considers composite geophysical logs from three wells SB1, SB2 and SB3 penetrated in Eastern Niger Delta field. The well log data comes in LAS format and contains gamma ray, resistivity, neutron and density logs. Schlumberger's Petrel 2018 Version Software was used for the processing and analysis of data. Some of the formation parameters were obtained using Equations 1 to 6.

Determination of Gamma Ray Index (IGR)

The gamma-ray log may be used to identify lithologies. Shale-free sandstones have low concentrations of radioactive material resulting in low gamma-ray readings. Increase in the shale content in the formation leads to an increase in the gamma-ray log- response due to the high concentration of radioactive materials. Equation 1 was adequate for this finding (Schlumberger, 1974; Atat *et al*., 2024a).

$$IGR = \frac{GR_{log} - GR_{min}}{GR_{max} - GR_{min}} \quad (1)$$

Where GR_{log} is the measured gamma ray log reading

GR_{min} is the minimum gamma-ray log reading in clean sand

GR_{max} is the maximum gamma-ray log reading in clean shale

Determination of shale volume (V_{sh})

The shale volume is a necessary parameter if effective porosity information is to be obtained; it may be calculated from the gamma-ray index (IGR) using Dresser (1979) formula (Equation 2) (Atat *et al*., 2024b).

$$V_{sh} = 0.083\left(2^{(3.7IGR)} - 1\right) \quad (2)$$

Determination of porosity

Porosity **($\emptyset_D$)** may be seen as the ratio of volume of empty space (pore volume) to the volume of rock (bulk volume) in a formation; it may be expressed in fraction (Equation 3) or percentage (Schlumberger, 1989; Umoren et al., 2023; Umoren et al., 2024; Akpabio et al., 2023a). It can be used to account for how much fluid a rock can hold (Akpabio et al., 2023b). It is calculated from density, sonic or neutron logs.

$$\emptyset_D = \frac{\rho_{ma} - \rho_b}{\rho_{ma} - \rho_f} \quad (3)$$

Where $\emptyset_D =$ total porosity

$\rho_{ma} =$ density of rock matrix = 2.65 g/cm³ for sandstone

$\rho_b =$ measured or bulk density

$\rho_f =$ fluid density; taken as 0.85 for oil and 0.2 for gas

The effective porosity ($\emptyset_{eff}$) was achieved using Equation 4. It may also be obtained using Asquith and Gibson (1982) recommendation.

$$\emptyset_{eff} = (1 - V_{sh})\emptyset_D \quad (4)$$

Where V_{sh} is the volume of shale.

Alternatively, the true porosity can be estimated using Equation 5. The combination of density and neutron logs, along with appropriate porosity estimation techniques, enhances the reliability of porosity and permeability determination in geological formations (Wood, 2020). They recommended Equation 6 which relates effective porosity to the cementation factor and tortuosity factor (George et al., 2024).

$$\phi = \sqrt{\frac{\phi_n^2 + \phi_d^2}{2}} \quad (5)$$

Where: ϕ represents the true porosity, ϕ_n and ϕ_d denote the neutron and density porosities, respectively.

$$\emptyset = \left(\frac{a\rho_w}{\rho}\right)^{1/m} \quad (6)$$

Where m is cementation factor and a is tortuosity factor, ρ_w is water resistivity and ρ is the bulk resistivity (George et al., 2024).

Shale and dirty sand are usually associated with high gamma ray response, while clean sand shows low gamma ray response due to the presence of radioactive minerals. Gamma ray was also used to measure grain size variation and subsequently inferring depositional energy and environment; resulting in the identified symmetrical and cylindrical physio-morphological display of the log motifs. Shale volume of various identified facie shapes was calculated to double check the cleanness of the identified sand units. The application of resistivity log delineates lithology and identify litho-fluid contacts of these wells; SB1 and SB3 were correlated based on the identified associated lithofacies.

A petrel project was created, data loaded and quality checked before analysis. Figure 3 shows the workflow for the study. The three wells were placed against each other and reduced to the same scale and sea level to facilitate correlation and assessment of data quality. Quantitative analysis of the log data was carried out to derive petrophysical parameters for lithology and fluids contact discrimination. The gamma ray log responses provide indication of facies shapes that were used to infer the different stratigraphic patterns and infer environments of deposition for interpretation.

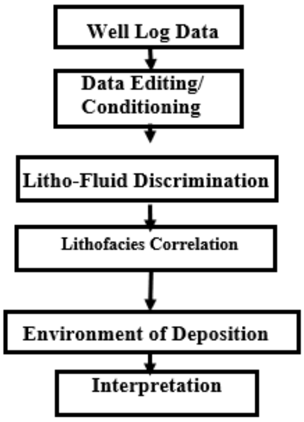

Figure 3: Workflow for the Study

3. Presentation of Results

The results of the study are presented in Tables 1 to 3 and Figures 4 to 16.

Table 1: Quantitative Basic log Parameters of Lithofacies for Well SB1

Curve		Gamma Ray	Neutron	Resistivity	Porosity	Volume of Shale
Unit		API	Dec	Ωm	%	Dec
Symmetrical (S1) (Top:5584ft, Bottom: 5624.5 ft, Net: 41 ft)	Min	19.40	0.14	5.921	0.14	0.06
	Max	68.16	0.40	837.04	0.40	0.22
	Mean	41.24	0.30	216.88	0.30	0.13
Cylindrical (C1) (Top:6363ft, Bottom: 6403.5ft, Net: 41ft)	Min	14.55	0.27	27.29	0.27	0.04
	Max	52.37	0.33	487.67	0.33	0.17
	Mean	19.86	0.30	202.30	0.30	0.06
Cylindrical (C2) (Top:6915.5ft, Bottom: 6943.5ft, Net: 28.5ft)	Min	13.56	0.08	6.70	0.29	0.04
	Max	87.47	0.34	864.83	0.34	0.29
	Mean	26.30	0.13	264.91	0.32	0.08

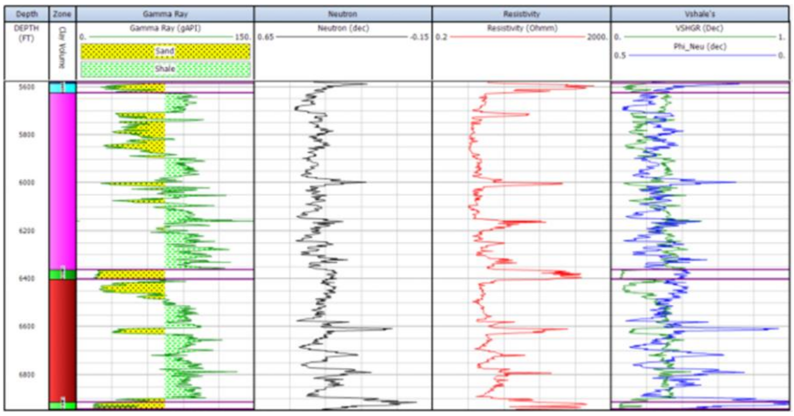

Figure 4: Basic well log Signatures for Well SB1

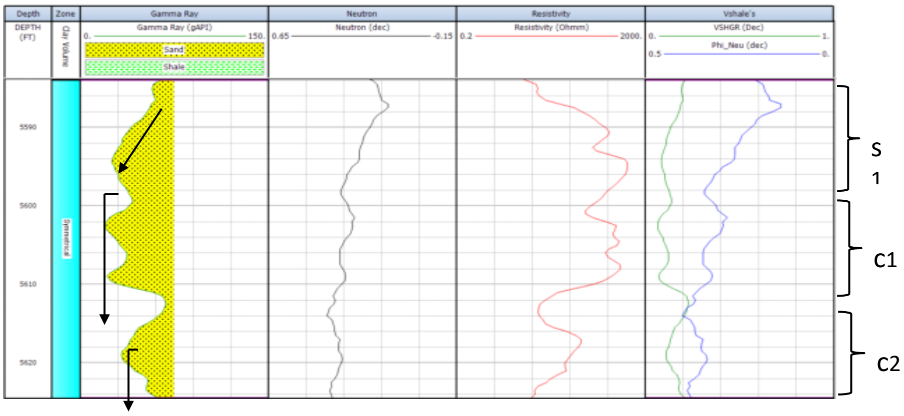

Figure 5: Dominant Sy mmetrical Shape facies of Well SB1

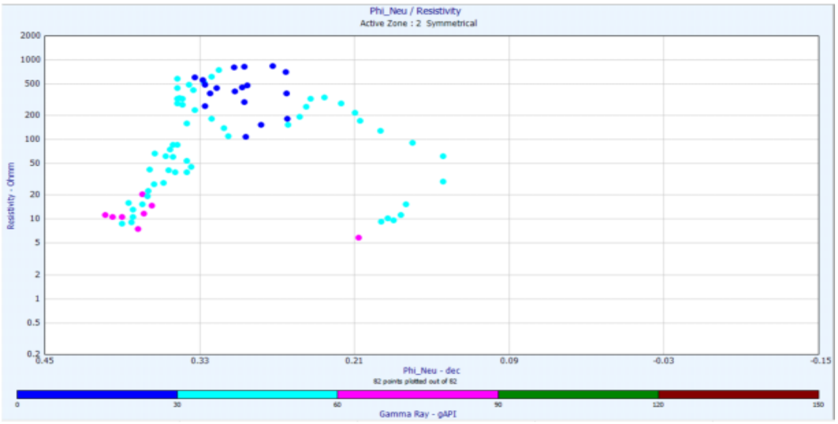

Figure 6: Resistivity versus Porosity Cross-plot of Well SB1

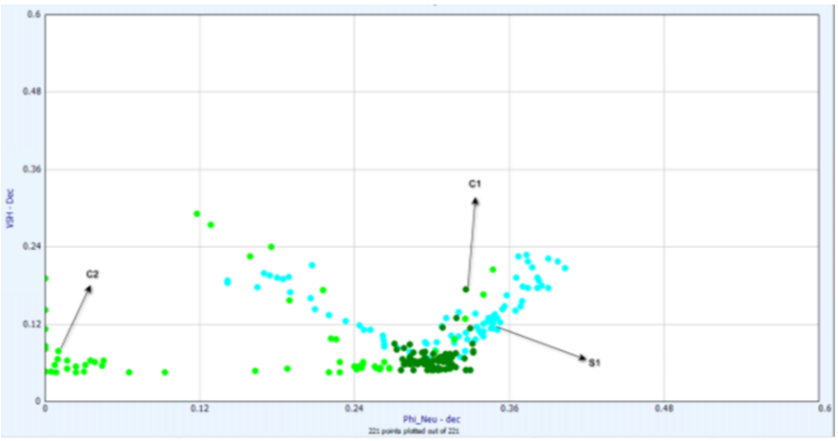

Figure 7: Vsh versus Porosity Cross-plot for Lithology of Well SB1

Table 2: Quantitative Basic log Parameters of Lithofacies for Well SB2

Curve		Density	Gamma Ray	Neutron	Resistivity	Porosity	Volume of Shale
Unit		g/c3	gAPI	Dec	Ohmm	%	Dec
Funnel F1(Top:5616.5 ft, Bottom:5661.5 ft, Net: 45.5 ft)	Min	2.06	14.41	0.26	3.46	0.26	0.04
	Max	2.23	67.99	0.41	346.21	0.41	0.27
	Mean	2.09	38.66	0.32	75.9	0.32	0.12
Cylindrical C1(Top:6380.5ft, Bottom: 6390.5ft, Net: 10.5ft)	Min	2.08	23.66	0.23	9.56	0.23	0.08
	Max	2.14	63.05	0.31	118.37	0.31	0.21
	Mean	2.10	32.01	0.27	83.15	0.27	0.11
Funnel F2(Top:6955ft, Bottom: 6985ft, Net: 30.5ft)	Min	2.09	14.73	0.15	2.16	0.15	0.05
	Max	2.24	70.01	0.303	40.3	0.30	0.23
	Mean	2.14	33.87	0.23	9.42	0.23	0.11

Figure 8: Basic Well Log signatures for Well SB2

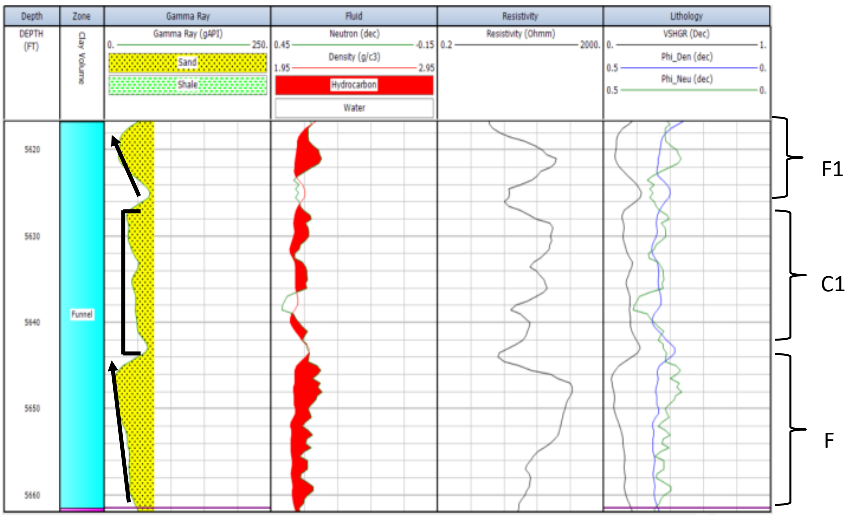

Figure 9: Dominant Funnel Shape facies of Well SB2

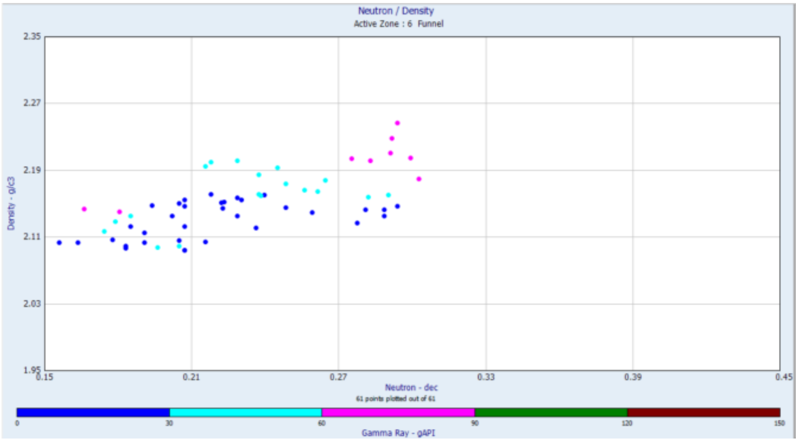

Figure 10: Density versus Porosity Cross-plot of Well SB2

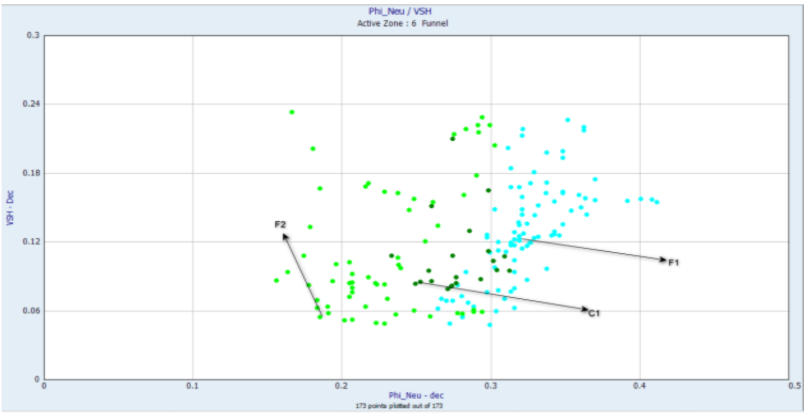

Figure 11: Vsh versus Porosity Cross-plot of Well SB2

Table 3: Quantitative Basic log Parameters of Lithofacies for Well SB3

Curve		Gamma Ray	Neutron	Resistivity	Porosity	Volume of Shale
Unit		API	Dec	Ω-m	%	Dec
Symmetrical (S1) (Top: 5612.5 ft, Bottom: 5664.5 ft, Net: 52.5 ft)	Min	20.97	0.25	1.74	0.25	0.06
	Max	74.22	0.41	1123.77	0.41	0.49
	Mean	43.07	0.30	131.23	0.30	0.24
Cylindrical (C1) (Top:6393.5ft, Bottom: 6405ft, Net: 12ft)	Min	18.84	0.25	1.82	0.25	0.04
	Max	59.37	0.29	182.04	0.29	0.37
	Mean	26.26	0.27	49.08	0.27	0.10
Cylindrical (C2) (Top: 6929.5ft, Bottom: 6960.5ft, Net: 31.5ft)	Min	18.06	0.18	2.95	0.18	0.03
	Max	72.45	0.27	95.52	0.27	0.47
	Mean	32.91	0.22	35.02	0.22	0.15

Figure 12: Basic Well Log Signatures for Well SB3

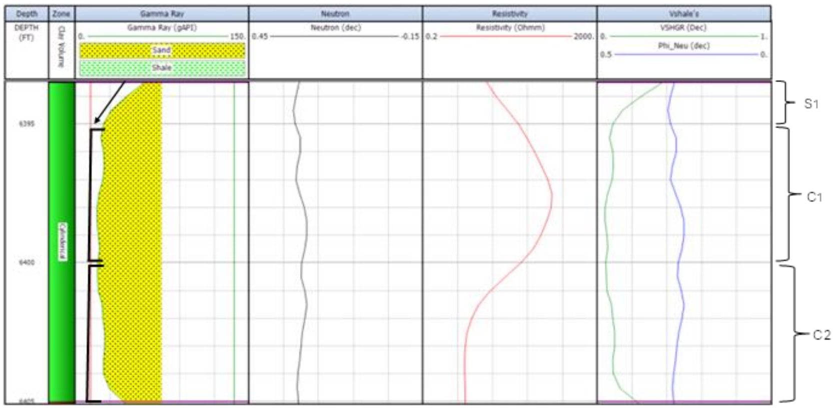

Figure 13: Dominant Cylindrical Shape facies of Well SB3

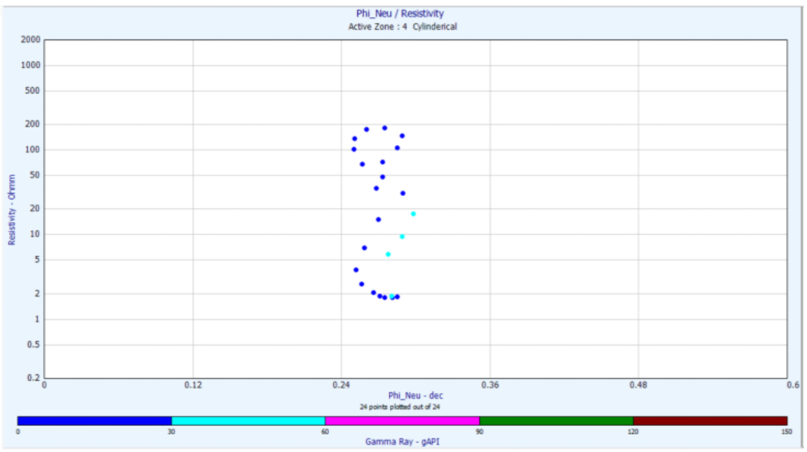

Figure14: Resistivity versus Porosity Cross-plot for Well SB3

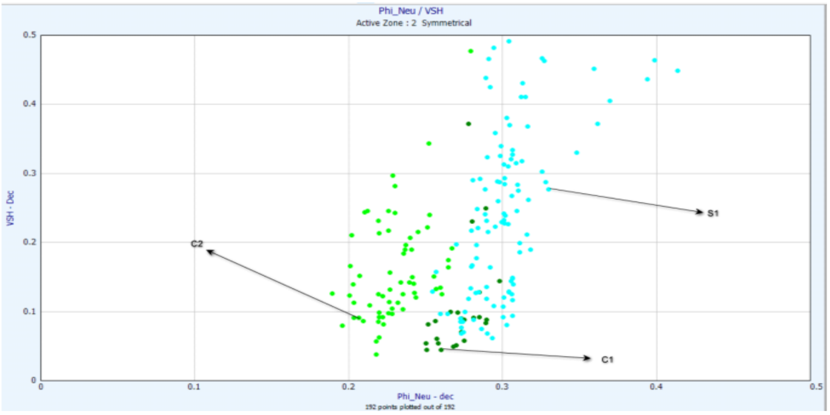

Figure 15: Vsh versus Porosity Cross-plot for Well SB3

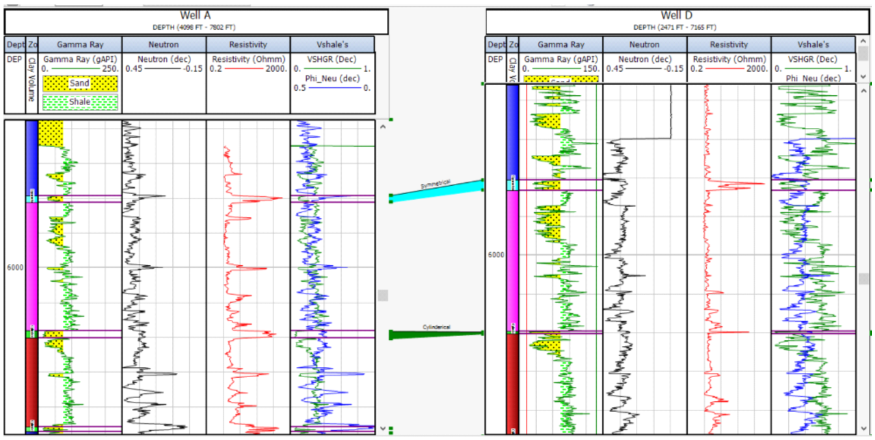

Figure 16: Stratigraphic Correlation of Wells SB1 and SB3

4. Discussion and Interpretation of Results

Tables 1, 2 and 3 show quantitative well log analysis of different parameters across the wells SB1, SB2 and SB3 respectively that give rise to lithofacies and fluid variability in the study area. There is a significantly marked relationship in the log signatures across the wells as indicated by Figures 4, 8 and 12 where the physiography of lithologies indicate occasional intercalations of sand/shale units. In the stratigraphy of the Niger Delta, this alternation of sand/shale bodies fall within the Akata-Agbada Formations which are of fluvio-marine and coastal origin with dominant shales and turbiditic sands. They confirms facie shapes indicated in Figures 5, 9 and 13 that predominantly comprise symmetrical, cylindrical and funnel shape facies; gradual coarsening downward and gentle fining downward indicating Low System Tract (LST) sequence of prograding to retrograding pattern of reworked offshore bar sands deposited during transgressive and regressive episodes (Udoh et al., 2020). Figure 13 is a cylindrical shape facie with sharp top and base and no significant variation in radioactive content, indicating clean sand unit deposited in an aggrading stacking pattern. The funnel shape coarsening upward sequence of shoreface-delta front, coarse to fine grained submarine sediments in a prograding depositional environment. The observed log shape depicts a strong pattern of coarsening upward progressing to fining downward with a sharp peak of High System Tract (HST). This pattern shows a progressive decline in gamma ray reactivity, indicating a low energy environment with laminar flow. The constant properties of this log shape give vital information on the variability of lithology.

Low to high variation in petrophysical properties across the area indicate good to excellent hydrocarbon accumulation potentialities. The high values in resistivity (up to 1123.77 Ω-m); porosity (up to 41%); low to moderate gamma value accompanied with low values in volume of shale, density and neutron logs show properties of good reservoir sand. (Avseth and Mukerji, 2002; Eze, 2014; Bello *et al*., 2015 and Austin *et al*., 2018). The litho-fluid crossplot in Figures 6, 10 and 14 for wells SB1, SB2 and SB3 respectively. According to the study, validate the sensitivity of lithofacies to discriminate reservoir fluid saturation condition, as indicated by resistivity-neutron crossplots (Figures 6 and 14) (Udo et al., 2017; Agbasi et al., 2018). The resistivity-porosity crossplot discriminates different fluids (oil, gas, water) have distinct resistivity-porosity relationship. Anomalies identified is an indication of potential hydrocarbon bearing intervals. The density-porosity cross-plot (Figure 10) discriminate different rock types (sandstones, shale, dolomite) with distinct density-porosity relationship and defined fluid saturation. In a related study, the volume of shale and the corresponding increase in porosity in wells SB1 and SB3 is probably due to increase in grain sizes and consequent decrease in gamma rate counts (Essien et al., 2017; Udoh et al., 2020). In well SB2 (Figure 10), cross-plot of density versus porosity for litho-fluids discrimination reveals the same trend of reservoir property of potential hydrocarbon accumulation.

Across the three wells, Figures 7, 11 and 15 show that consideration of porosity and volume of shale data points on a cross-plot reflect a broad range of low shale volume with the corresponding moderate to high porosity values, which suggest the presence of good reservoir sands. The Vsh-porosity crossplot helps in identifying the impacts of shale on reservoir quality and estimating net-to-gross which is essential for reservoir volumetrics. The scattered points represent lithologic differences within the field as supported by (Nwagwu et al., 2019). The dispersion of data points in the cross-plots shows low to average value of 0.04 to 0.5; and 0.13 to 0.42 volume of shale in agreement with (Bello et al., 2015; Austin et al., 2018). Generally, the average porosity values (22% to 32%) indicate that the formations are in the good to excellent class with the ability to transmit and store fluid; the mean shale volume values (6% to 24%) show that the reservoir is over 70% clean sand formation which supports free fluid migration (Atat et al., 2022; Atat et al., 2024a). However, submitting differently, the intermittent variability in lithofacies and lithologies is not unconnected with the discrete velocities of different grain sizes during transportation and subsequent differential drag forces during deposition. This lithology variations might affect the reservoir fluids flow parameters, such as permeability and interconnectivity.

Figure 16 shows stratigraphic correlation between Wells SB1 and Well SB3. The association is to compare and match the geological and sedimentary features detected in both wells. Similar patterns of sedimentary and lithological changes were found within facie shapes in both wells. These facies are distinguished by a balanced arrangement of sedimentary deposits with uniformly dispersed coarser and finer sand units. The facies correlation implies similar depositional environment, with the occurrence of comparable geological processes; sediment sources; and the prevailing conditions at the time of deposition and subsequent diagenetic processes. These facies have sedimentary strata that are cylindrical in form with identifiable geometry and continuity of sand units. The correlation shows continuity of sand deposits between wells SB1 and SB3, implying a shared sedimentary history and depositional environment. A more thorough knowledge of the geological properties and sedimentation processes in the area is accomplished by correlating wells SB1 and SB3 along the symmetrical and cylindrical form facies. This connection assists in the interpretation of subsurface strata, thus makes reservoir mapping easier, thereby leads to a better knowledge of regional stratigraphic study.

5. Conclusion

The application of gamma ray, neutron, resistivity and density logs to determine porosity, volume of shale and litho-fluid crossplot has characterized the lithofacies and reservoir properties of the study area as a good hydrocarbon prospect.

The well correlation study between wells SB1 and SB3 reveal information on the facies association and continuity between the two wells. The connection indicates similarities in sedimentary facies as well as lithological alterations between the symmetrical and cylindrical trends. This link reflects a similar depositional environment, which implies similar geological processes and sediment sources. On the overall, the detailed examination of lithology and porosity characteristics in Wells SB1, SB2 and SB3 add to a better understanding of the reservoir's composition, fluid content and rock properties. The results of the study improve reservoir characterization efforts and assist in making informed decisions for hydrocarbon exploration and production operations.

References

Agbasi, E. O., Chukwu, G. U., Igboekwe, M.U and Etuk, S. E., 2018. Pore fluid and lithology discrimination of a well in the Niger Delta region using elastic parameters. World News of Natural Science, 17, 75-88.

Akpabio, I. O., Atat, J. G., Akankpo, A. O., 2023b. Local Fit Parameter Satisfying Shear Modulus Porosity Relation for Southern Z Basin Analysis. Neuroquantology, 21(5), Pp. 1385-1391.

Akpabio, I. O., Atat, J. G., Umoren, E. B., Ekemini, J. D., 2023a. The reservoir rock volumetric concentration and tortuosity description of pore space of Xa field, Niger Delta Basin. World Journal of Advanced Science and Technology, 03(01), Pp. 001 – 013.

Akpabio, I. O., Ejedawe, J. and Ebinero, J., 2013. Thermal state of the Niger Delta Basin. Proceedings of the 38th Workshop on Geothermal Reservoir Engineering, Standford, Carlifonia.

Akpabio, I. O., Ejedawe, J. E., Ebinero, J. O., and Uko, E. D., 2003. Geothermal gradients in Niger Delta basin from continuous temperature logs. Global Journal of Pure and Applied Sciences, 9(2), Pp. 265-271.

Asquith, G. B. and Gibson, C. R., 1982. Basic Well Log Analysis for Geologists. The American Association of Petroleum Geologists (AAPG), Tulsa.

Atat, J. G., Akpabio, I. O. and Ekpo, S. S., 2022. Percentile-Oqive Approach Determines the Textural Parameters of X_a Field Lithology and the Suitable Technique for Porosity Estimates. Current Science, 2(5), Pp. 230 – 240.

Atat, J. G., Umoren, E. B., Akankpo, A. O. and Patrick, N. A., 2024b. An Information on Ps Field Reservoir Worth Using Well Log Data in the Niger Delta Basin, Global Journal of Engineering and Technology (GJET), 3(6), Pp. 1 – 7.

Atat, J. G., Umoren, E. B., Akpabio, I. O. Akankpo, A. O. and Enoh, R. E., 2024a. Investigation of the Zeta Field Reservoir Rock and Fluid Transport Properties, Niger Delta Basin. Malaysian Journal of Geosciences (MJG), 8(1), Pp. 46 – 58.

Austin, O.E. Agbasi, O.E., Onyekuru, S. and Etuk, S. E., 2018. Crossplot analysis of rock properties from well log data for gas detection in Soku Field, Coastal Swamp Depobelt, Niger Delta Basin. Journal of Geoscience, Engineering, Environment and Technology, 3(4), Pp. 180-186.

Avseth, P. and Mukerji T., 2002. Seismic lithofacies classification from well logs using statistical rock physics. Petrophysics. 43, Pp. 70-81.

Bello, R., Igwenagu, C. L. and Onifade, Y. S., 2015. Cross plotting of rock properties for fluid and lithology discrimination using well data in a Niger Delta Oil Field. Nigerian Journal of Physics, 19(3), Pp. 539 – 546.

Boggs, S., 2006. Principles of Sedimentology and Stratigraphy. Pearson Prentice hall, USA, p. 622.

Doust, H. and Omatsola, E., 1990. Niger Delta, In: Edwards J. D. and Santogrossi, P.A, (Editors) Divergent/Passive Margin Basins, American Association of Petroleum Geologists, Tulsa. Pp. 239-248.

Dresser Atlas, 1979. Log Interpretation Charts; (Houston, Dresser Industries. Inc.,).

Ejedawe, J. E., 1989. The Eastern Niger Delta: geological evolution and hydrocarbon occurrences. SPDC Internal Bulletin, 7(2), Pp. 11-18.

Emery, D. and Mayers, K. J., 1996. Sequence stratigraphy. Blackwell Science Limited, Oxford, p. 289.

Essien, U. E., Akankpo, A.O. and Agbasi, O.E., 2017. Evaluation of reservoirs Petrophysical parameters, Niger Delta, Nigeria. International Journal of Advance Geosciences, 5, Pp. 9-25.

Eze, C. C., 2014. Using lame petrophysical parameters for fluid detection and lithology determination in parts of Niger Delta. Global Journal of Geological Sciences, 13, Pp. 23-33.

George, N. J., Ekanem, A. M., Thomas, J. E., Udosen, N. I., Ossaib, N. M. and Atat, J. G., 2024. Electro-Sequence Valorization of Specific Enablers of Aquifer Vulnerability and Contamination: A Case of Index-Based Model Approach for Ascertaining the Threats to Quality Groundwater in Sedimentary Beds. HydroResearch, 7, Pp. 71–85.

Nuhu, R., Sani, A. M. and Yandoka, B. M. S., 2019. Depositional environment and sequence stratigraphyof tertiary sediments of Oleum field, Eastern Niger Delta Basin Nigeria. Journal of Pure and Applied Sciences, 17, Pp. 61-72.

Nwagwu, E. A., Emujakporue, G. O., Ugwu, S. A. and Oghonya, R., 2019. Lithofacies and depositional environment from geophysical logs of EMK Field, Deepwater Niger Delta, Nigeria. Current Research in Geoscience, 9, Pp. 1-9.

Okoli, E. A., Edward, A. J. and Ngozi, E. C., 2020. Interpretation of depositional environment, Rho Field using sequence stratigraphic analysis, shallow offshore depobelt, Niger Delta. Journal of Scientific Research and Reports, 26(1), Pp. 93-103.

Oyedele, K. F., Oladele, S., Ogagarue, D. O. and Bakare, K., 2012. Sequence stratigraphic approach to hydrocarbon exploration in Bobsaa field, Onshore Niger Delta. Journal of Petroleum and Gas Exploration Research, 2(6), Pp. 106-114.

Reijers, T. J. A., 2011. Stratigraphy and sedimentology of the Niger Delta. Geologos, 17(3), Pp. 133-162.

Schlumberger, 1974. Log Interpretation. Volume-II-Principles; (Houston, Schlumberger Well Services Inc.,).

Schlumberger, 1989. Log interpretation, principles and application: Schlumberger Wireline and Testing, Houston, Texas, pp. 21-89.

Udo, K. I., Akpabio, I. O. and Umoren, E. B. 2017. Derived rock attributes analysis for enhanced reservoir fluid and lithology discrimination. Journal of Applied Geology and Geophysics, 5, Pp. 95-105.

Udoh, A. C., Bassey, C. E., Ekot, A. E. and Udoh, M. U., 2020. Sequence stratigraphic study of X field in Eastern offshore of Niger Delta, Nigeria. Journal of Geology and Mining Research, 12(2), Pp. 65-79.

Umoren, E. B., Atat, J. G., Akankpo, A. O. and Usen, I. C., 2023. Porosity Estimation Using RHG Approach and Well Log Data from Southern Niger Delta, Nigeria. World Journal of Applied Science and Technology, 15(2), Pp. 207 – 212.

Umoren, E. B., Atat, J. G., Akankpo, A. O., Uzoewulu, R. O. (2024). Determination of Permeability and Velocity Information of Oil Reservoir Using Well Log Data (S-Field). Malaysian Journal of Geosciences (MJG), 8(2), Pp. 47 – 52.

Wood, D. A., 2020. Predicting Porosity, Permeability and Water Saturation Applying an Optimized Nearest-Neighbour, Machine-Learning and Data-Mining Network of Well-Log Data. Journal of Petroleum Science and Engineering, 184, 106587.